SEMI-EMPIRICAL MO STUDY OF REACTIONS MODELLING BIOCHEMICAL OXIDATION OF ETHANOL*

Jiří Krechl and Josef Kuthan

Department of Organic Chemistry,
Prague Institute of Chemical Technology, 166 28 Prague 6

Received October 22nd, 1981

The EHT, CNDO/2 and INDO methods have been used to find the energetically most favourable arrangement of the supermolecules 1-methylnicotiniumamide cation (*I*) — ethanol (*II*), *I* — ethoxide anion (*III*) and 1-methyl-1,4-dihydronicotinamide (*IV*) — protonated acetaldehyde (*V*). An attempt has been made to define with more precision these geometries with the use of the gradient optimization based on CNDO/2 wave functions. Quantum-chemical characteristics of the studied systems are discussed with respect to possible course of biochemical reactions.

The low-molecular components involved in the chemical transformations catalyzed by alcoholdehydrogenases can be summarized in six molecular structures *I* to *VI* where the formulas *I* and *IV* represent the oxidized and reduced forms of pyridine nucleotide, respectively. They participate in the corresponding chemical reactions (from the point of view of summary equations) as follows:

$$I + II \rightleftharpoons IV + V, \quad \text{or} \qquad (A)$$

$$I + III \rightleftharpoons IV + VI. \qquad (B)$$

The reaction (*A*) necessitates deprotonation of the oxidized ethanol molecule *II* in the process of the catalyzed reaction, whereas the reaction (*B*) is a closer model of the oxidation of the pre-deprotonated substrate *III*. The most recent findings[1,2] about structure of the active centre support the existence of the reacting substrate *II* in a form close to the anion *III* bound to a zinc atom, but the nature of this coordination in the course of the reaction has not yet been fully elucidated, so the processes (*A*) and (*B*) deserve closer theoretical investigation.

Examination of energy relations of the two equilibria (*A*) and (*B*) by means of quantum chemistry requires energy calculation for four supermolecules: *I*–*II*,

* Part XVIII in the series On Calculations of Biologically Important Compounds; Part XVII: Int. J. Quantum Chem. *21*, 1029 (1982).

I—III, *IV—V* and *IV—VI*. In our previous communications[3,4] we used the EHT and CNDO/2 methods for investigation of the *IV—VI* supermolecule (in a simplified case R = CH_3), and we found some mutual orientations of the two partners *IV* and *VI* which appeared energetically favourable from the point of view of the said semi-empirical MO calculations. In the present communication the mentioned MO studies are extended to the remaining three supermolecules *I—II*, *I—III* and *IV—V* with the same simplification, *i.e.* R = CH_3. Recent studies[5,6] concerning also the MO approach to reactivity of dehydrogenases (particularly that of lactatedehydrogenase) considered it unnecessary to involve explicitely the coenzyme components *I* and *IV*, respectively, stressing the representation of influence of molecular structure of the other components of the active centre. Our approach can be considered complementary to the above-mentioned one.

CALCULATIONS

On the whole, we carried out 384 EHT, 246 CNDO/2 and 10 INDO calculations. They were carried out on an ICL-4-72 computer with the use of standard programs. The parameters used for the calculations were the same as those of refs[3,4]. Geometry of the compound *I* was chosen in accordance with ref.[7], that of *II* and *III* according to ref.[8]. Geometry of *IV* component was chosen the same as in the reports[3,4], for the *V* component we used the energetically most favourable structure found by comparison of several alternative *ab initio* calculations in 4—31 G base[9]. As the studied supermolecules can be considered as containing the prochirality elements, it is necessary to characterize the orientation of the attacking molecule with respect to the attacked one and thus specify more closely the chosen configurational types. For nomenclature of the latter we used the Hanson suggestion[10] given in a clear survey[11,12]. In the cases *IV—V* and *IV—VI* we always considered the attack of substrate on the *proR* hydrogen atom *H*(4′) of dihydropyridine ring of *IV*. In the cases *I—II* and *I—III* the substrate attack was directed to *re*-face of the quaternay nicotinamide *I*. Orientation of the substrates with respect to the heterocycles *IV* and *I* is denoted as it follows: if the molecule *V* and *VI*, respectively, approaches the heterocycle *IV* by its *re*-face, the situation is denoted with symbol (*a*); if the molecule *V* and *VI*, respectively, is oriented to the heterocycle *IV* by its *si*-face, then symbol (*b*) is used. When evaluating the interaction type of the molecule *II* and *III*, respectively, with quaternary nicotinamide *I*, it is obvious that, with respect to C(4) position of *I*, the molecule *II* and *III*, respectively, can be oriented either by its *proS* hydrogen atom (H′) or by its *proR* hydrogen atom (H″). The former configurational type, *i.e.* attack of the heterocycle by the *proR* hydrogen centre H′, bears the symbol (*c*), the latter one, *i.e.* attack by the *proS* hydrogen H″, has the symbol (*d*). From the point of view of the used simple quantum-chemical model it is unimportant to deal with the other configurational series in which *proS* hydrogen atom of *IV* and *si*-face of *I*, respectively, are attacked, because the resulting characteristics are identical with those of the above configurational series. The starting arrangement of the supermolecules *I—II* and *I—III* is given in Fig. 1*A*: the heterocycle in *xy* plane, the C(4) atom in the origin of coordinates, the C(4)—H(4′) bond in positive *y* semi-axis. The C_a—C_b bond of *II* (or *III*) molecule was parallel with *y* axis, the methyl group at C_b was directed outside the heterocycle plane, the hydrogen atoms at C_a were situated in *xz* plane, their perpendicular distance from *xy* plane was 200 pm. The geometry parameters were varied within the limits: $0\,0 \leqq \Delta r \leqq 100$ pm; $0\,0 \leqq \Delta s \leqq 100$ pm; $0° \leqq \alpha \leqq 60°$; $0° \leqq \beta \leqq 360°$ with the iterations 10 pm and 10 to 20°, respectively (Fig. 1*A*). Total energy was calculated for each combination of all four geometry parameters.

RESULTS AND DISCUSSION

Supermolecules I–II and I–III, the EHT calculations. Typical dependences of the EHT energies on one geometry parameter (the other parameters being constant) according to the situations in Fig. 1 are represented in Figs 2 and 3. By evaluation of all the energies it was found that the starting arrangement is energetically preferred for both the supermolecule *I–II*(*c*) and the system *I–III*(*c*) (*i.e.* the arrangement with $\Delta r = \Delta s = 0$ pm; $\alpha = \beta = 0°$). This trivial conclusion is obviously due to the fact that the EHT method, which neglects the electron repulsion, is not able to reflect electrostatic interaction of charged molecules, and, therefore, it qualifies changes of geometrical arrangement of the supermolecules *I–II* and *I–III* as sterically unfavourable. The EHT characteristics of the both supermolecules were compared for this arrangement. The energy of *I–II*(*c*) supermolecule is by 369 kJ mol^{-1} (*i.e.* approximately by dissociation energy of O—H bond) lower than that of *I–III*(*c*) at the same geometrical arrangement. Characteristics of frontier orbitals of the EHT wave function are given in Table I. From the table it follows that in the both cases the LUMO is distinctly localized at C(4) position of the heterocycle, *i.e.* at a key position of biochemical reduction.

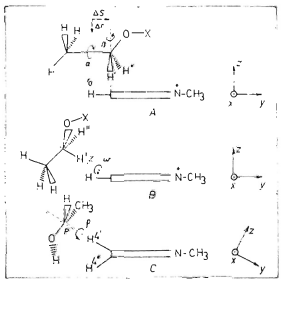

FIG. 1

Survey of the starting arrangements of the supermolecules studied *A* The starting arrangement of the supermolecules *I–II* (X = H) and *I–III* (X ≅ free electron pair) for the configurational types (*c*) and (*d*). Δr vertical shift of the molecules *II* or *III* towards the ring plane; Δs horizontal shift of the molecules *II* or *III* above the ring plane; α rotation of the molecules *II* or *III* around the C_a—C_b bond; β rotation of the molecules *II* or *III* around the axis connecting the C_a and C(4) centres; r_0 the starting distance of H(C_a) hydrogen from the plane of the heterocycle *I*. *B* The starting arrangement of the supermolecules *I–II* (X = H) and *I–III* (X ≅ free electron pair) for the configurational types (*c'*) and (*d'*). *z* distance between the H(C_a) and C(4) centres; ω rotation of the molecules *II* or *III* around the connecting line of the H(C_a) and C(4) centres. *C* The starting arrangement of the *IV–V* supermolecule. *p* distance between the C(=O) and (H4') centres; ϱ rotation of the molecule *V* around the connecting line of the C(=O) and H(4') centres

To enable comparison of configurationally similar cases, the CNDO/2 calculations of *I—III* and *I—II* supermolecules used the arrangements analogous to those of the

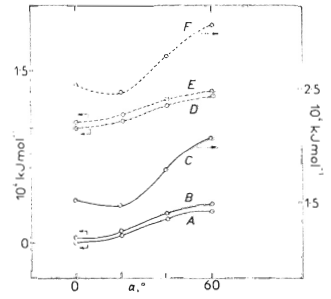

FIG. 2

Dependence of the total EHT energies of the supermolecules *I—II* (curves *A—C*), *I—III* (curves *D—F*) on the rotation parameter α. Curve *A*: $\Delta r = 50$ pm, $\Delta s = 50$ pm, $\beta = 0°$; *B*: $\Delta r = 50$ pm, $\Delta s = 100$ pm, $\beta = 0°$; *C*: $\Delta r = 100$ pm, $\Delta s = 0$ pm, $\beta = 60°$; *D*: $\Delta r = 50$ pm, $\Delta s = 50$ pm, $\beta = 0°$; *E*: $\Delta r = 50$ pm, $\Delta s = 100$ pm, $\beta = 0°$; *F*: $\Delta r = 100$ pm, $\Delta s = 0$ pm, $\beta = 60°$

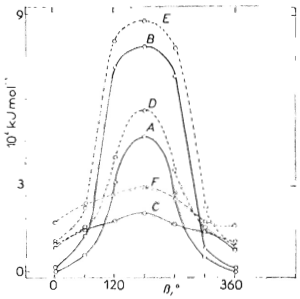

FIG. 3

Dependence of the total EHT energies of the supermolecules *I—II* (curves *A—C*) and *I—III* (curves *D—F*) on the rotation parameter β. Curve *A*: $\Delta r = 50$ pm, $\Delta s = 50$ pm, $\alpha = 20°$; *B*: $\Delta r = 50$ pm, $\Delta s = 100$ pm, $\alpha = 20°$; *C*: $\Delta r = 100$ pm, $\Delta s = 0$ pm, $\alpha = 60°$; *D*: $\Delta r = 50$ pm, $\Delta s = 50$ pm, $\alpha = 20°$; *E*: $\Delta r = 50$ pm, $\Delta s = 100$ pm, $\alpha = 20°$; *F*: $\Delta r = 100$ pm, $\Delta s = 0$ pm, $\alpha = 60°$

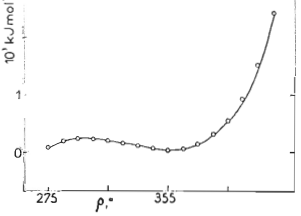

FIG. 4

Dependence of the total $E_{CNDO/2}$ energy of the *IV—V*(*a*) supermolecule on the rotation parameter ϱ for $p = 170$ pm

above EHT calculations (Fig. 1*A*), and rotation of the molecule around the C_a—C_b axis was considered in such a way that atom H' (in *I*—*III*(*d*) and *I*—*II*(*d*) geometries) or H" (in *I*—*III*(*c*) and *I*—*II*(*c*) geometries) approached to C(4) carbon centre of the

TABLE I

The expansion coefficients of the EHT wave functions $|c_i| \geqq 0{\cdot}1$ for the *I*—*II*(*c*) and *I*—*III*(*c*) supermolecules for $\Delta r = \Delta s = 0{\cdot}0$ pm, $\alpha = \beta = 0{\cdot}0°$

I—*II*(*c*)				*I*—*III*(*c*)			
HOMO		LUMO		HOMO		LUMO	
C_a PX	−0·18	C(3) PZ	0·31	C(2) PZ	0·44	C(3) PZ	0·31
$O(C_a)$ PX	0·15	C(4) PZ	−0·59	C(3) PZ	0·42	C(4) PZ	−0·59
H" S	−0·10	C(5) PZ	0·55	C(5) PZ	−0·41	C(5) PZ	0·54
C(2) PZ	0·44	C(6) PZ	0·47	C(6) PZ	−0·44	C(6) PZ	0·47
C(3) PZ	0·42	N(1) PZ	−0·37	N(3') PZ	−0·21	N(1) PZ	−0·37
C(5) PZ	−0·41	N(3') PZ	−0·30	C_a PX	−0·18	N(3') PZ	−0·30
C(6) PZ	−0·44	O(3') PZ	−0·25	$O(C_a)$ PX	0·15	O(3') PZ	−0·25
N(3') PZ	−0·22			H" S	−0·10		

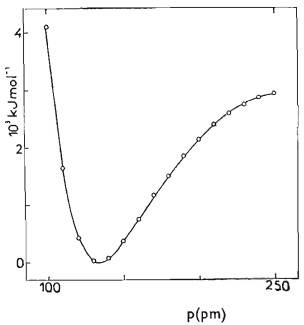

FIG. 5

Dependence of the total $E_{CNDO/2}$ energy of the *IV*—*V*(*a*) supermolecule on the translation parameter *p* for $\varrho = 355°$

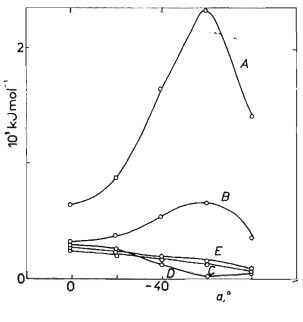

FIG. 6

Dependence of the total $E_{CNDO/2}$ energy of the *I*—*II*(*d*) supermolecule on the rotation parameter α. Curve A: $r_0 = 180$ pm; B: $r_0 = 200$ pm; C: $r_0 = 220$ pm; D: $r_0 = 240$ pm; E: $r_0 = 260$ pm

heterocycle. Another configurational type denoted as (*c'*) or (*d'*) was arranged in such way that hydrogen atom at C_a of substrate was directed towards the C(4) centre of the heterocycle, and connecting line of these centres formed with plane of the quaternary heterocycle *I* the same angle as the C(4)—H(4') bond with the plane of the heterocycle *IV* did. From schematic representation it is seen that transfer of a reduction equivalent H'' (for (*c'*) geometry) or H' (for (*d'*) geometry) to C(4) position of the heterocycle and mere rotation transform the system into the configuration denoted as *IV*–*VI* or *IV*–*V*, respectively.

Supermolecule IV–V, *the* CNDO/2 *calculations.* The starting arrangement of the supermolecule (Fig. 1*C*) for the configurational type (*a*) was chosen on the basis

TABLE II

Changes in distribution of the CNDO/2 and INDO charge in the *IV*–*V*(*a*) and *IV*–*VI*(*a*) supermolecules related to the isolated molecules, $p = 170$ pm, $\varphi = 325°$

	Centre	CNDO/2 . 10^5		INDO . 10^5	
		IV–*V*(*a*)	*IV*–*VI*(*a*)[a]	*IV*–*V*(*a*)	*IV*–*VI*(*a*)[a]
	H(4')	−4 662	2 539	−4 108	2 323
	H(4'')	2 255	742	2 685	736
	C(3)	−1 807	2	−940	−79
IV	C(4)	2 825	−1 529	1 519	−1 198
	C(5)	−2 276	−215	−1 241	−265
	C(3')	−511	−108	−440	−4
	O(3')	3 244	−209	3 415	−238
	N(3')	−309	−430	−588	−460
	H(—C)	−1 828	—	3 125	—
	C(=O)	−921	—	−12 845	—
V	$C(H_3)$	1 241	—	6 285	—
	O(=C)	−4 580	—	−2 732	—
	H(—O)	−2 451	—	−2 735	—
	H(—C)	—	−592	—	2 757
VI	C(=O)	—	2 934	—	−5 718
	$C(H_3)$	—	−337	—	3 242
	O(=C)	—	−4 373	—	−1 414
	Total *V*	−8 539	—	−8 902	—
	Total *VI*	—	−2 310	—	−2 450

[a] The values for the *IV*–*VI*(*a*) supermolecule according to ref.[4].

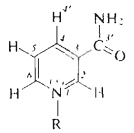

I

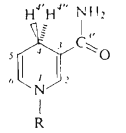

IV

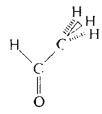

VI

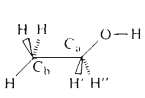

II

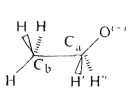

III

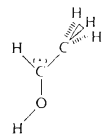

V

of the geometry found in the previous communication[4]. First we investigated that arrangement of the *IV*–*V*(*a*) supermolecule which was found[4] most favourable for the case of the neutral molecules arranged in the *IV*–*VI* supermolecule. Acetaldehyde (*VI*) was replaced by the protonated form *V*, and the CNDO/2 and INDO calculations were carried out. Table II compares the CNDO/2 and INDO charges of the non-protonated system *IV*–*VI*(*a*) and the protonated system *IV*–*V*(*a*) related to the isolated molecules. From Table II it is obvious that in the protonated system *IV*–*V*(*a*) a much more important transfer of negative charge to acetaldehyde takes place (involving especially its carbonyl carbon atom) than in the non-protonated system. This fact could indicate a possible course of biochemical reduction *via* the protonated substrate. A similar comparison of the CNDO/2 wave functions for the two systems in Table III indicates that, whereas in the non-protonated system the both frontier orbitals – HOMO and LUMO – are distributed over the whole supermolecule, in the case of the protonated supermolecule *IV*–*V*(*a*) the LUMO is practically exclusively localized at carbonyl group of acetaldehyde. This fact can be interpreted in such way that excitation into the LUMO could be iniciated by radiation at the beginning of the reduction. Further we varied the geometry parameters p and ϱ with the aim of finding the change of the optimum mutual arrangement of *IV* and *V* due to protonation. From Fig. 4 it is seen that the dependence of the total energy $E_{\mathrm{CNDO}/2}$ on the rotation parameter ϱ shows a very indistinct minimum for $\varrho = 355°$. But further rotation of the component *V* increases the energy steeply, which is obviously due to sterical hindrance to movement of methyl group in ion *V* and heterocycle *IV*. Moreover, we examined dependence of the total energy $E_{\mathrm{CNDO}/2}$ on the p parameter for the mentioned energy minimum at $\varrho = 355°$. From Fig. 5 it follows that in the protonated supermolecule *IV*–*V*(*a*) there is a somewhat smaller equilibrium distance of the two

components, *viz.* $p = 130$ pm (*cf.* $p = 170$ pm for the non-protonated $IV-VI(a)$ system[4]). For the optimum arrangement of $IV-V(a)$ supermolecule found in this way we again examined the CNDO/2 wave function and compared the CNDO/2 and INDO electron characteristics. The results are summarized in Tables IV and V. Although this arrangement is somewhat preferred energetically, the LUMO is not so unambiguously localized at carbonyl group of *V*. Similarly, it must be stated that, in contrast to the arrangement 170 pm and 325°, in the case of 130 pm and 355° a more marked charge transfer to the *V* molecule is observed. As the system $IV-VI$ was judged[4] in two configurational types (*a*) and (*b*), in this case we also verified energetical advantages of the opposite arrangement $IV-V(b)$. In the same way (*i.e.* by rotation according to the ϱ parameter and translation according to p parameter) we found the optimum conformation of the $IV-V(b)$ supermolecule. In this case the energetically most favourable conformation can be described by the parameters $\varrho = 335°$ and $p = 140$ pm. In this arrangement, the tested form $IV-V(b)$ has a higher energy than the $IV-V(a)$ supermolecule by 1·25 kJ mol^{-1}.

TABLE III

Expansion coefficients of the CNDO/2 wave function $|c_i| \geqq 0{\cdot}1$ for the $IV-V(a)$ and $IV-VI(a)$ supermolecules, $p = 170$ pm, $\varrho = 325°$

HOMO						LUMO					
$IV-VI(a)$[a]			$IV-V(a)$			$IV-VI(a)$[a]			$IV-V(a)$		
H(4′)	S	0·25	H(4′)	S	−0·23	N(1)	PY	−0·15	C(=O)	PY	−0·80
H(4″)	S	−0·24	H(4″)	S	0·23	N(1)	PZ	−0·11	O(=C)	PY	0·37
N(1)	PY	0·46	N(1)	PY	−0·47	C(2)	PY	0·51			
N(1)	PZ	0·33	N(1)	PZ	−0·33	C(2)	PZ	0·36			
C(2)	PY	−0·18	C(2)	PY	0·15	C(3)	PY	−0·32			
C(2)	PZ	−0·13	C(3)	PY	0·35	C(3)	PZ	−0·22			
C(3)	PY	−0·35	C(3)	PZ	0·26	C(5)	PY	0·15			
C(3)	PZ	−0·24	C(5)	PY	0·27	C(5)	PZ	0·10			
C(4)	PY	0·14	C(5)	PZ	0·20	C(6)	PY	−0·10			
C(5)	PY	−0·27	C(6)	PY	0·11	C(3′)	PY	−0·32			
C(5)	PZ	−0·18	O(3′)	PY	−0·27	C(3′)	PZ	−0·22			
C(6)	PY	−0·15	O(3′)	PZ	−0·18	O(3′)	PY	0·27			
C(6)	PZ	−0·11	C(=O)	PY	0·13	O(3′)	PZ	0·19			
O(3′)	PY	0·24	O(=C)	PY	−0·11	N(3′)	PY	0·16			
O(3′)	PZ	0·17				N(3′)	PZ	0·10			
O(=C)	PY	0·14				C(=O)	PY	−0·16			
						O(=C)	PY	0·15			

[a] Values for the $IV-VI(a)$ supermolecule according to ref.[4].

The I−II *and* I−III *supermolecules, configurations* (c) *and* (d), CNDO/2 *calculations.* The starting arrangement was chosen the same as the best EHT geometry, and only two geometry parameters (r_0 and α) were varied (Fig. 1*A*). The *I*−*II*(*d*) and *I*−*III*(*d*) supermolecules appear intuitively to be somewhat more probable than their (*c*) forms, because in the natural enzyme in this arrangement the oxygen atom has more space for a bond to the zinc atom incorporated in the complex system of amino acids[13]. The question is whether the relatively simple model which we have chosen

TABLE IV

Expansion coefficients of the CNDO/2 wave function $|c_i| \geqq 0{\cdot}1$ for the *IV*− *V*(*a*) supermolecule, $p = 130$ pm, $\varrho = 355°$

HOMO			HOMO			LUMO		
H(4′)	S	0·21	C(5)	PY	−0·26	N(1)	PY	−0·13
H(4″)	S	−0·21	C(5)	PZ	−0 20	C(2)	PY	0·14
N(1)	PY	0·48	O(3′)	PY	0·30	C(2)	PZ	0·13
N(1)	PZ	0·32	O(3′)	PZ	0·19	C(4)	S	−0·19
C(2)	PY	−0·13	C(=O)	PY	−0·18	C(4)	PY	−0·37
C(3)	PY	−0·35	O(=C)	PY	0·14	C(6)	PZ	0·10
C(3)	PZ	−0·26				C(=O)	PY	−0·74
						O(=C)	PY	0·28

TABLE V

Changes in distribution of the CNDO/2 and INDO charge in the *IV*− *V*(*a*) supermolecule related to the isolated components, $p = 130$ pm, $\varrho = 355°$

	Centre	CNDO/2[a]	INDO[a]		Centre	CNDO/2[a]	INDO[a]
	H(4′)	2 496	3 203		H(—C)	−4 071	385
	H(4″)	4 376	5 083		C(=O)	−5 081	−15 141
	C(3)	−1 904	706		$C(H_3)$	1 548	6 168
I	C(4)	4 336	2 037	*V*	O(=C)	−10 359	−9 852
	C(5)	−2 636	1 277		H(—O)	−5 041	−4 935
	C(3′)	−889	−212				
	O(3′)	4 032	17 117				
	N(3′)	−908	−1 223				

[a] The charge values $\times 10^5$.

is able to confirm this consideration. Figs 6 and 7 give dependences of the total CNDO/2 energy on the r_0 and α parameters for the supermolecules *I*–*II*(*d*) and *I*–*II*(*d*), respectively. Repulsive interaction predominates at small distances of the two components in the supermolecule, but at a sufficient distance, on the contrary, rotation is preferred resulting in greater proximity of the H′ atom at C_a of the *II* (or *III*) molecule and nicotinamide cation. Energetically the most favourable are the configurations $r_0 = 240$ pm, $\alpha = -60°$ (for *I*–*II*(*d*) supermolecule) and $r_0 = 190$ pm, $\alpha = -60°$ (for *I*–*III*(*d*)). Tables VI and VII give electron distribution and wave function at these points. For the *I*–*III*(*d*) supermolecule the energy course exhibits (at lower distances of the two components) a steep energy increase at the passage of the H′ atom over C(4) position of the heterocycle (see curves *E* and *F* in

TABLE VI

Changes in distribution of CNDO/2 and INDO charge in the *I*–*II*(*d*) supermolecule for $r_0 = 240$ pm, $\alpha = -60°$, and *I*–*III*(*d*) for $r_0 = 190$ pm, $\alpha = -60°$, related to the isolated molecules

	Centre	*I*–*II*(*d*)		*I*–*III*(*d*)	
		CNDO/2 . 10^5	INDO . 10^5	CNDO/2 . 10^5	INDO . 10^5
	N(1)	−1 058	1 010	−10 167	−10 160
	C(2)	403	341	548	303
	C(3)	−1 228	−1 213	−6 803	−7 111
	C(4)	2 639	2 805	8 466	9 354
I	C(5)	−982	−947	−4 273	−4 529
	C(6)	355	267	−22	−60
	C(3′)	41	45	369	556
	N(3′)	−124	−157	−491	−729
	O(3′)	−187	−148	−4 569	−4 274
	H′(C_a)	−2 623	−2 804	—	—
II	C_a	−903	−882	—	—
	C_b	−428	−462	—	—
	O	1 432	1 575	—	—
	H′(C_a)	—	—	11 077	10 289
III	C_a	—	—	68	−1 373
	C_b	—	—	−1 392	−979
	O	—	—	11 794	13 154
	Total *II*	−2 522	−2 573	—	—
	Total *III*	—	—	21 547	21 091

Fig. 7), *i.e.* at a position corresponding probably to key location for the reduction equivalent transfer. From Table VI it follows that, in the case *I*–*II*(*d*), the expected

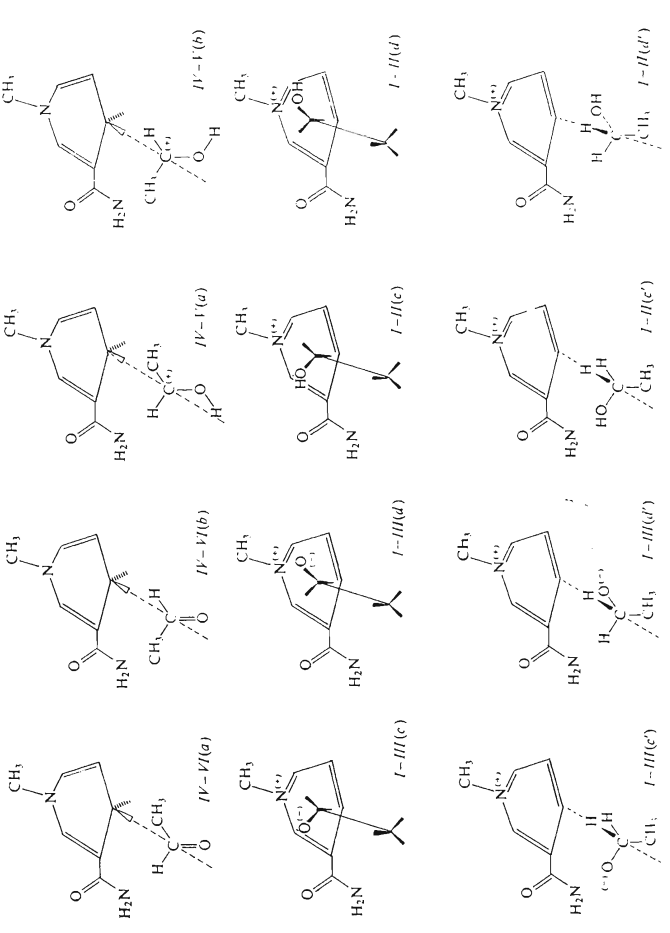

TABLE VII

Expansion coefficients of the CNDO/2 wave function $c_i \geqq 0.1$ for the supermolecules $I-II(d)$, $r_0 = 240$ pm, $\alpha = -60°$, and $I-III(d)$, $r_0 = 190$ pm, $\alpha = -60°$

$I-II(d)$					$I-III(d)$				
HOMO			LUMO		HOMO			LUMO	
H′(C_a)	S	0·19	C(2)	PZ 0·37	H′(C_a)	S	−0·34	H′(C_a)	S 0·22
C(2)	PZ	−0·11	C(3)	PZ 0·17	C(2)	PZ	0·15	C(2)	PZ 0·38
C(3)	PZ	−0·18	C(4)	PZ −0·56	C(3)	PZ	0·18	C(4)	PZ 0·55
C(4)	PZ	−0·15	C(6)	PZ 0·47	C(4)	PZ	−0·16	C(6)	PZ 0·44
C(6)	PZ	0·10	N(1)	PZ −0·50	C(5)	PZ	0·16	N(1)	PZ −0·39
C(3′)	PZ	0·19			C(6)	PZ	0·14	C_a	S 0·10
N(1)	PZ	0·12			N(1)	PZ	−0·24	C_a	PZ −0·24
N(3′)	PZ	−0·55			C_b	PY	−0·13	O(C_a)	PZ 0·21
O(3′)	PZ	0·64			O(C_a)	PX	−0·19		
C_a	PZ	−0·17			O(C_a)	PY	−0·41		
O(C_a)	PZ	0·21			O(C_a)	PZ	−0·66		

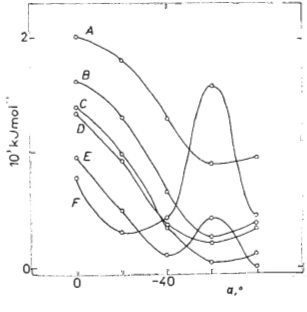

FIG. 7

Dependence of the total $E_{CNDO/2}$ energy of the $I-III(d)$ supermolecule on the rotation parameter α. Curve A: $r_0 = 220$ pm; B: $r_0 = 200$ pm; C: $r_0 = 190$ pm; D: $r_0 = 180$ pm; E: $r_0 = 170$ pm; F: $r_0 = 160$ pm

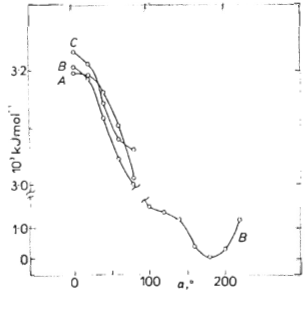

FIG. 8

Dependence of the total $E_{CNDO/2}$ energies of the $I-II(c)$ supermolecule on the rotation parameter α. Curve A: $r_0 = 220$ pm; B: $r_0 = 240$ pm; C: $r_0 = 260$ pm

charge transfer from ethanol *II* to quaternary nicotinamide *I* is not observed; on the contrary, there is even a slight increase of negative charge in ethanol *II*. However, in the case of the $I-III(d)$ supermolecule, a distinct transfer of electrons from ethoxide anion *III* to quaternary nicotinamide *I* can be observed (as compared with the isolated molecules) especially so from the H' and O centres of the molecule *III*. The transferred negative charge neutralizes preferently the positive charge at N(1) nitrogen. Analysis of the wave function in Table VII shows that in both $I-II(d)$ and $I-III(d)$ the LUMO is distinctly localized in the region about C(4) of the heterocycle *I*. The HOMO of $I-II(d)$ is delocalized over the whole heterocycle *I* and partially also on the *II* molecule (at H' atom), but the HOMO of $I-III(d)$ is preferently localized in the molecule of substrate *III*, especially at its key hydrogen atom H'. From the two said findings a conclusion can be drawn that the deprotonated system $I-III(d)$ is markedly more able to carry out the oxidation-reduction step than the $I-II(d)$ system. This conclusion is supported by the considerable charge transfer from substrate *III* to the coenzyme model *I* and by the localization of the frontier orbitals HOMO and LUMO favourable for the reaction step. At the same time, we also

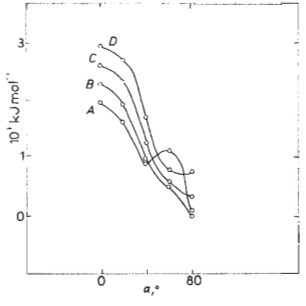

FIG. 9

Dependence of the total $E_{CNDO/2}$ energies of the $I-III(c)$ supermolecule on the rotation parameter α. Curve A: $r_0 = 170$ pm; B: $r_0 = 180$ pm; C: $r_0 = 190$ pm; D: $r_0 = 200$ pm

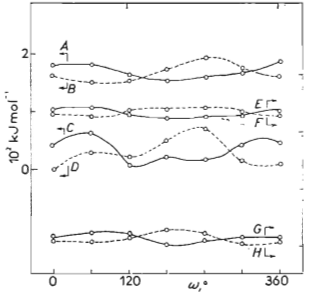

FIG. 10

Dependences of the total $E_{CNDO/2}$ energies of the supermolecules $I-II$ and $I-III(c')$ and (d') on the rotation parameter ω. Curve A: $I-II(d')$, $z = 300$ pm; B: $I-II(c')$, $z = 300$ pm; C: $I-II(d')$, $z = 200$ pm; D: $I-II(c')$, $z = 200$ pm; E: $I-III(d')$, $z = 300$ pm; F: $I-III(c')$, $z = 300$ pm; G: $I-III(d')$, $z = 200$ pm; H: $I-III(c')$, $z = 200$ pm

verified the alternative arrangement (*c*). The changes of the CNDO/2 energy with changing r_0 and α parameters are represented in Figs 8 and 9 for *I*–*II*(*c*) and *I*–*III*(*c*) supermolecules, respectively. The energy courses do not much differ for the types (*c*) and (*d*). Whereas rotation in the *I*–*II*(*d*) supermolecule has its energy optimum at $\alpha = -60°$ (just corresponding to eclipsed position of H′ and C(4)), the *I*–*II*(*c*) and *I*–*III*(*c*) supermolecules prefer further rotation up to the value $\alpha = 180°$. This, of course, brings the hydrogen centre H″ out of the position favourable for a direct attack on the C(4) atom of *I*. The driving force of this phenomenon comes obviously from electrostatic attraction of the electron pair at oxygen of *II* positively charged heterocycle *I*. An interesting course shows curve A in Fig. 9 which exhibits considerable repulsive action for $\alpha = 60°$ (*i.e.* for the H″ atom located against C(4) centre). The fact that the supermolecules *I*–*II*(*c*) and *I*–*III*(*c*) (in contrast to *I*–*II*(*d*) and *I*–*III*(*d*)) are not stabilized in a position suitable for transition of a reduction equivalent enables a conclusion that this arrangement is not suitable for the reduction steps (*A*) and (*B*).

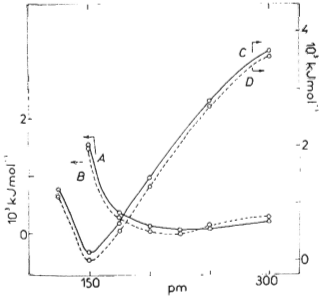

FIG. 11

Dependence of the total $E_{CNDO/2}$ energies of the *I*–*II* and *I*–*III* supermolecules (*c*′) and (*d*′) on the translation parameter *z*. Curve A: *I*–*II*(*d*′), $\omega = 240°$; B: I–II(*c*′), $\omega = 300°$; C: *I*–*III*(*d*′), $\omega = 120°$; D: *I*–*III*(*c*′), $\omega = 300°$

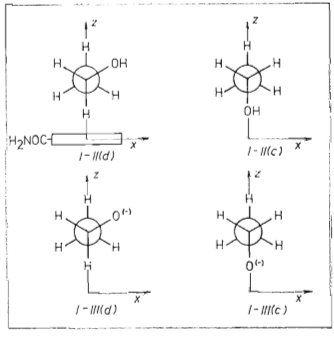

FIG. 12

Schematical representation of localization of the optimum arrangements of the *I*–*II* and *I*–*III* supermolecules (*c*) and (*d*) in the coordinate system

It is obviously useful to look for still closer geometry relationships between the *I—II* and *IV—V* supermolecules and *I—III* and *IV—VI* supermolecules. Therefore, another series of CNDO/2 calculations was carried out in which the space arrangement of the *II* and *III* molecules approached the optimum orientation of the *V* and *VI* molecules, respectively, in the *IV—V* and *IV—VI* supermolecules already solved. This arrangement is schematically represented in Fig. 1*B*. The C_a—H bond aimed at the C(4) centre of the heterocycle *I* under the same angle which would be formed (during transition of a reduction equivalent) between the C(4)—H(4′) bond and plane of the heterocycle *IV*. In this way we examined the possibilities denoted as (*c′*) and (*d′*) for the both supermolecules *I—II* and *I—III*. Mutual orientation of the two components of the supermolecules was varied according to ω and *z* parameters (Fig. 1*B*). The dependence of the CNDO/2 energies on these parameters is given in Fig. 10. Rotations of the molecules *II* and *III* show substantially lower energy barriers than in the case of the above-discussed parallel arrangement. The parameter ω was adjusted, and the optimum value for the parameter z was looked for. The dependences CNDO/2 energy *vs z* parameter for various values of ω parameter are given in Fig. 11. It is seen that the energy depends more distinctly on the distance of the

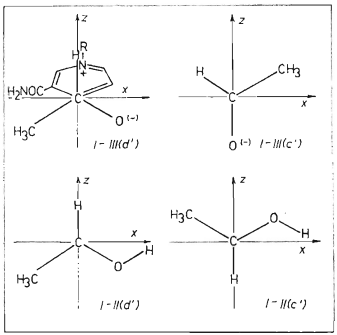

FIG. 13

Schematical representation of localization of the optimum arrangements of the *I—II* and *I—III* supermolecules (*c′*) and (*d′*) in the coordinate system

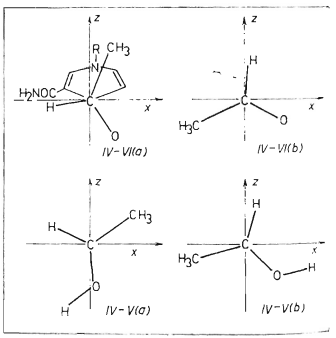

FIG. 14

Schematical representation of localization of the optimum arrangements of the *IV—V* and *IV—VI* supermolecules (*a*) and (*b*) in the coordinate system. The arrangements *IV* to *VI*(*a*) and *IV—VI*(*b*) according to ref.[4]

two components than on their mutual rotations (Fig. 10), and does not depend much on choice of the configurational type; the (*c'*) arrangement is somewhat better. Stabilization of the *I* and *III* components with opposite charges is substantially stronger than that of the combination of quaternary nicotinamide *I* with neutral molecule *II*. The optimum arrangement of the *I*–*II*(*c'*) supermolecule can be described by the parameters $\omega = 300°$ and $z = 225$ pm; for the *I*–*II*(*d'*) case: $\omega = 240°$, $z = 225$ pm; *I*–*III*(*c'*): $\omega = 300°$, $z = 150$ pm; *I*–*III*(*d'*): $\omega = 120°$, $z = 150$ pm. For the optimum arrangements of the *I*–*II* and *I*–*III* supermolecules type (*c'*) and (*d'*) found in this way we analyzed the CNDO/2 and INDO charge distributions and wave functions of the frontier orbitals HOMO and LUMO. Comparison of Tables VIII and IX with Table VI shows that for *I*–*II*(*c'*) and *I*–*II*(*d'*) a slight transfer of negative charge can be observed from *II* to *I* molecule, whereas the opposite is true for the *I*–*II*(*d*) case. However, the negative charge transfer is smaller for

TABLE VIII

Changes in distribution of the CNDO/2 charge ($\times 10^5$) in the optimum arrangement of the *I*–*II* and *I*–*III* supermolecules (*c'*) and (*d'*) related to the isolated components

	Centre	*I*–*II*(*d'*)	*I*–*II*(*c'*)	*I*–*III*(*d'*)	*I*–*III*(*c'*)
	N(1)	−251	−282	−7 786	−7 798
	C(2)	−154	91	151	−157
	C(3)	−226	−301	−4 773	−4 323
	C(4)	582	511	3 936	4 459
	C(5)	−277	−306	−3 765	−4 184
I	C(6)	119	89	−836	−661
	C(3')	34	−27	692	866
	N(3')	−108	−64	−137	481
	O(3')	−19	−134	−4 852	−5 204
	H(—C_a)	−3 307	706	—	—
II	C_a	3	104	—	—
	C_b	−311	−383	--	—
	O	874	923	—	—
	H(—C_a)	—	—	6 292	5 337
III	C_a	—	—	362	522
	C_b	—	—	−1 366	−1 062
	O	—	—	9 691	9 282
	total *II*	−2 741	135	—	—
	total *III*	—	—	14 979	14 079

I–*III*(*c'*) and *I*–*III*(*d'*) than for *I*–*III*(*d*). Comparison of expansion coefficients of wave functions of the frontier orbitals HOMO and LUMO for the *I*–*II* and *I*–*III*(*c'*) and (*d'*) supermolecules inTable X shows that in the *I*–*III*(*c'*) and *I*–*III*(*d'*) supermolecules the HOMO is distinctly localized in *III*, substantial portion of the LUMO being at C(4) centre, which is not true of the *I*–*II*(*c'*) and *I*–*II*(*d'*) supermolecules.

Table XI compares energies of all the supermolecules investigated. The *IV*–*V* and *IV*–*VI* supermolecules are strikingly more favourable energetically as compared with *I*–*II* and *I*–*III* supermolecules. This difference is especially marked with the *I*–*III* supermolecules in which the redistribution of charges of the originally neutral *IV*–*VI* system, giving the *I*–*III* system with separated centres of positive and negative charge, leads to a steep increase of the energy of system. This fact could indicate that

TABLE IX

Changes in distribution of the INDO charge ($\times 10^5$) in the optimum arrangement of the *I*–*II* and *I*–*III* supermolecules (*c'*) and (*d'*) related to the isolated components

	Centre	*I*–*II*(*d'*)	*I*–*II*(*c'*)	*I*–*III*(*d'*)	*I*–*III*(*c'*)
	N(1)	−24	−271	−7 795	−7 774
	C(2)	142	71	−228	−56
	C(3)	−236	−309	−4 892	−4 308
	C(4)	638	574	4 285	493
I	C(5)	−295	−317	−3 826	−4 345
	C(6)	104	70	−1 217	−1 003
	C(3')	43	−26	773	975
	N(3')	−156	−154	−206	568
	O(3')	−3	−130	−4 686	−5 121
	H(—C_a)	−3 227	656	—	—
II	C_a	15	152	—	—
	C_b	3 842	−437	—	—
	O	907	1 008	—	—
	H(--C_a)	—	—	6 122	5 158
	C_a	—	—	−653	−380
III	C_b	—	—	−1 138	−720
	O	—	—	11 214	10 543
	total *II*	1 537	1 379	—	—
	total *III*	—	—	15 545	14 601

the reactions (*A*) and (*B*) would go faster from left to right (*i.e.* in favour of oxidation of the substrate) in spite of no energy barriers being known along the respective reaction coordinates. Finally it must be decided what is the orientation of the oxidized substrate *II* or *III* with respect to the coenzyme model. From the point of view of the energy arrangement given in Table XI as well as the above-discussed quantum-chemical characteristics given in Tables VI and VII to X it can be concluded that the most favourable arrangement of the *I*–*II* and *I*–*III* supermolecules is that designed by (*d*), *i.e.* parallel arrangement of the substrate and the coenzyme model. In contrast to (*c*) configuration, (*d*) affords enough space for further fixation of oxygen atom of

TABLE X

Expansion coefficients $|c_i| \geqq 0{\cdot}1$ of the frontier orbitals HOMO and LUMO for the optimum arrangement of the *I*–*II* and *I*–*III* supermolecules (*c'*) and (*d'*)

I–*II*(*d'*)			*I*–*II*(*c'*)			*I*–*III*(*d'*)			*I*–*III*(*c'*)		
					HOMO						
H′(C_a)	S	0·13	H″(C_a)	S	−0·11	H′(C_a)	S	0·33	H′(C_a)	S	0·13
C(2)	PY	−0·11	C(2)	PY	0·11	H″(C_a)	S	−0·12	H″(C_a)	S	−0·33
C(3)	PZ	−0·10	C(3′)	PY	−0·15	C(3)	PY	−0·12	C(3)	PY	0·12
C(3′)	PY	0·15	C(3′)	PZ	−0·14	C(4)	PY	0·12	C(4)	PY	−0·11
C(3′)	PZ	0·14	N(3′)	PY	0·48	C(5)	PY	−0·10	C(4)	PZ	−0·11
N(3′)	PY	−0·47	N(3′)	PZ	0·40	N(1)	PY	0·15	C(5)	PY	0·10
N(3′)	PZ	−0·40	O(3′)	PY	−0·59	N(1)	PZ	0·11	N(1)	PY	−0·16
O(3′)	PY	0·59	O(3′)	PZ	−0·31	C_b	PX	0·10	N(1)	PZ	−0·11
O(3′)	PZ	0·30	O(C_a)	PY	−0·12	O(C_a)	PY	0·79	C_b	PX	0·10
C_a	PY	−0·11				O(C_a)	PZ	0·27	O(C_a)	PX	0·27
O(C_a)	PY	0·15							O(C_a)	PY	−0·79
					LUMO						
C(2)	PY	−0·30	C(2)	PY	−0·30	H′(C_a)	S	−0·20	H″(C_a)	S	−0·19
C(2)	PZ	−0·21	C(2)	PZ	−0·21	C(2)	PY	−0·32	C(2)	PY	−0·31
C(3)	PY	−0·15	C(3)	PY	−0·15	C(2)	PZ	−0·23	C(2)	PZ	−0·23
C(3)	PZ	−0·10	C(3)	PZ	−0·10	C(4)	PY	0·45	C(4)	PY	0·45
C(4)	PY	0·45	C(4)	PY	0·45	C(4)	PZ	0·27	C(4)	PZ	0·27
C(4)	PZ	0·31	C(4)	PZ	0·31	C(6)	PY	−0·38	C(6)	PY	−0·38
C(6)	PY	−0·39	C(6)	PY	−0·39	C(6)	PZ	−0·27	C(6)	PZ	−0·27
C(6)	PZ	−0·28	C(6)	PZ	−0·28	N(1)	PY	0·35	N(1)	PY	0·35
N(1)	PY	0·41	N(1)	PY	0·41	N(1)	PZ	0·25	N(1)	PZ	0·25
N(1)	PZ	0·30	N(1)	PZ	0·30	C_a	PY	0·20	C_a	PY	0·20
						O(C_a)	PY	−0·20	O(C_a)	PY	−0·20

the substrate in the way known for the natural enzyme[13]. Figs 12 to 14 represent schematically localization of the optimum positions of the substrate molecules in coordinate system. The figures show a very good agreement in the pairs of configurations: $I-III(d')$ and $I-II(d')$, $IV-VI(a)$ and $IV-V(a)$, $IV-VI(b)$ and $IV-V(b)$, which can be interpreted by the fact that the optimum arrangements of the non-protonated geometries do not substantially differ from the protonated ones except for the pair (c) and (c'). Similar parallels can be found in the sense of Eqs (a) and (B) also between the pairs of supermolecules $IV-VI(a)$ and $I-III(c')$, $IV-VI(b)$ and $I-III(d')$, $IV-V(b)$ and $I-II(d')$. On the basis of energy preference and application of quantum-chemical characteristics to biochemical key centres of the examined systems, a presumption was made in the above text that the most favourable arrangements for the (A) and (B) processes from left to right are $I-II(d)$ and $I-III(d)$. However, the above-given comparison of the pairs of supermolecules indicates a possibility of the (A) and (B) reaction course without substantial change in geometry arrangement of the two partners forming the supermolecule.

Furthermore, Table XI reveals that the CNDO/2 stabilization energies of the considered supermolecules are relatively high due probably to overestimation of non-bonding interactions in the procedure used. Nevertheless, the above-discussed changes in electron distribution, particularly the charge transfer between the individual partners, could indicate already beginning bonding interactions in the optimized structures given in Table XI.

The given approach to the search for the optimum arrangement of the reactants on the basis of the model of rigid rotators could, of course, be carried out only in confrontation of the electrically charged and neutral supermolecules due to un-

TABLE XI

Comparison of the CNDO/2 relative and stabilization energies for the optimum arrangement of the superamolecules studied. All the data are in kJ mol^{-1}

Supermolecule	E_{rel}	E_{stab}	Supermolecule	E_{rel}	E_{stab}
$IV-VI(a)$	0·0[a]	−473·9	$IV-V(a)$	0 0	−312·2
$IV-VI(b)$	60·7[a]	−471·6	$IV-V(b)$	342·2	−299·6
$I-III(c)$	[b]	[b]	$I-II(c)$	[b]	[b]
$I-III(d)$	19 521·3	−461·3	$I-II(d)$	8 669·8	−227·2
$I-III(c')$	21 337·5	−394·6	$I-II(c')$	8 846·4	−16·2
$I-III(d')$	21 462·6	−390·0	$I-II(d')$	8 848·0	−16·1

[a] According to ref.[4]; [b] the supermolecule is not stabilized.

certainty in adequate representation of energy of the two types of systems within the limits of the CNDO/2 procedure. On the contrary, the nature of the real course of the reactions (*A*) and (*B*) in hydrophobic cavity of the corresponding enzyme made it possible to ignore completely the solvent effect.

REFERENCES

1. Eklund H., Nordström B., Zeppezauer E., Söderlund G., Ohlsson I., Boiwe T., Bränden C. I.: FEBS (Fed. Eur. Biochem. Soc.) Lett. *44*, 200 (1974).
2. Eklund H., Nordström B. O., Tapia O., Bränden C. I., Åkeson Å.: J. Mol. Biol. *102*, 27 (1976).
3. Krechl J., Kuthan J.: This Journal *45*, 2187 (1980).
4. Krechl J., Kuthan J.: This Journal *46*, 740 (1981).
5. Umeyama H., Imamura A., Nagata C., Nakagawa S.: Chem. Pharm. Bull. *25*, 1685 (1977).
6. Umeyama H., Nakagawa S.: Chem. Pharm. Bull. *28*, 2292 (1980).
7. Krechl J., Kuthan J.: This Journal *45*, 2194 (1980).
8. Pople J. A., Gordon M.: J. Amer. Chem. Soc. *89*, 4253 (1967).
9. DelBene J. E.: J. Amer. Chem. Soc. *100*, 1673 (1978).
10. Hanson K. R.: J. Amer. Chem. Soc. *88*, 2731 (1966).
11. Červinka O., Bláha K.: Chem. Listy *61*, 1028 (1967).
12. Červinka O.: Chem. Listy *61*, 1307 (1967).
13. Krechl J.: Chem. Listy *74*, 491 (1980).

Translated by J. Panchartek.